

## Ecological invasion: spatial clustering and the critical radius

Andrew Allstadt,<sup>1</sup> Thomas Caraco<sup>1\*</sup> and G. Korniss<sup>2</sup>

<sup>1</sup>*Department of Biological Sciences, University of Albany, Albany, NY 12222 and*  
<sup>2</sup>*Department of Physics, Applied Physics and Astronomy, Rensselaer Polytechnic Institute,*  
*110 8th Street, Troy, NY 12180-3590, USA*

---

### ABSTRACT

**Question:** When localized dispersal spatially aggregates an introduced species, so that an introduction's success or failure corresponds to growth or decay of invader clusters respectively, how does the probability of cluster expansion vary with propagation rates of locally interacting invaders and residents, with their mortality rates, and with dispersal distance?

**Mathematical method:** We apply the physical theory for nucleation in homogeneous spatial systems to invader–resident competition, and focus on an invader cluster's critical radius. At the critical radius, growth and decay of an invader cluster have equal probability. Using this definition, analytically and computationally, we explore the effects of individual-level vital rates on the probability of invader-cluster growth.

**Key assumptions:** The two species compete preemptively for space. Invader and resident have the same mortality rate, but the invader has the greater rate of local propagation. Invader clusters are (on average) circular, and advance or decline of the invader occurs at the cluster's perimeter.

**Conclusions:** The probability that an invader cluster grows, so that introduction succeeds, increases with an error function of the logarithm of the cluster's radius. Variation in lattice-neighbourhood size has little effect on cluster-growth probability in simulation. For small differences in propagation rates, increasing the common mortality rate increases the invader's critical radius, but may also increase the probability that large clusters invade the resident. That is, increased mortality hampers small invader clusters through chance extinction, but provides more opportunities for growth at the periphery of large clusters. The (approximate) critical radius of invader clusters scales as a power law of the difference in the two species' propagation rates.

*Keywords:* cluster growth, invasive species, nucleation theory, spatial competition.

### INTRODUCTION

Invasion analyses address the dynamics of rarity, and so integrate concepts common to ecology, evolution, and epidemiology (Ferriere and Gatto, 1995; Caraco *et al.*, 1998; Shea and Chesson, 2002;

---

\* Author to whom all correspondence should be addressed. e-mail: caraco@albany.edu  
Consult the copyright statement on the inside front cover for non-commercial copying policies.

White *et al.*, 2006). The study of ecological invasion has additional, practical significance; the breakdown of biogeographic barriers (Rosenzweig, 2001) has accelerated introductions of exotics, including species that endanger agriculture or native biodiversity (Pimm, 1987; Andow *et al.*, 1990; Pimentel *et al.*, 2000; Butin *et al.*, 2005).

Ecological invasion analyses identify conditions promoting growth of a rare, introduced species. The majority of exotic-species introductions apparently fail to generate invasive growth (Lonsdale, 1999; Simberloff, 2000; Cassey, 2003). Indeed, a series of failed introductions often precedes a species' successful introduction and subsequent advance (Veltman *et al.*, 1996; Sax and Brown, 2000). Lacking further detail, we take the outcome of any given introduction as uncertain (O'Malley *et al.*, 2005). Our study addresses one basis for this uncertainty. We model spatially detailed competition between an invader and a resident. The invader has the greater rate of local propagation, and hence has a per-individual advantage in competition for space. Propagation generates clustered growth, and we define an invader cluster's critical radius as follows. At the critical radius, growth and decay of the invader cluster are equally probable (Gandhi *et al.*, 1999; Korniss and Caraco, 2005; O'Malley *et al.*, 2005, 2006a). The critical-radius concept frames an understanding of the way variation in local demographic rates can govern the likelihood a given cluster increases in size or declines to extinction.

## SPATIAL COMPETITION AND CLUSTERED INVADERS

Biological invasions ordinarily exhibit spatial organization (Ellner *et al.*, 1998; Neubert *et al.*, 2000; Zadoks, 2000; Travis *et al.*, 2005). We observe spatially structured dynamics from highly localized (Frantzen and van den Bosch, 2000) to geographic scales (van den Bosch *et al.*, 1992; Butin *et al.*, 2005). Most theoretical analyses of spatial invasion restrict attention to successful introduction, emphasizing the asymptotic velocity of invasive advance (Dwyer and Elkinton, 1995; Kot *et al.*, 1996; Caraco *et al.*, 2002; O'Malley *et al.*, 2006b, in press). However, Lewis and Kareiva (1993) call attention to the fundamental ecological importance of the initial phase of spatial invasion, where introduction succeeds or fails (van Baalen and Rand, 1998; Lewis and Pacala, 2000; Thomson and Ellner, 2003). Given spatially aggregated growth, the introduction's success or failure equates with an invader cluster's expansion or decay to extinction (Gandhi *et al.*, 1999; O'Malley *et al.*, 2006a).

To begin our study of invader-cluster dynamics, we briefly summarize previous ecological analyses of the critical radius. Next we turn to nucleation theory and develop our conceptual approach to cluster growth under preemptive competition. We define an individual-based, probabilistic invasion model which assumes discrete space. Then we analyse a deterministic, geometric model for the critical radius. Finally, we test the geometric model's predictions in stochastic simulations of the growth and decay of invader clusters.

### Background: reaction-diffusion approximation

Two previous papers describe a critical radius for invasive growth. Lewis and Kareiva (1993) and Gandhi *et al.* (1999) apply reaction-diffusion approximations to the ecological dynamics of cluster growth. The first study considers a single invading species whose reproduction exhibits an Allee effect. The second study models two competing species where local propagation is frequency-dependent and mortality is density-dependent. Each analysis first calculates a planar wave speed, the velocity at which a linear front (cluster with an infinite radius) would advance. That velocity is corrected by the finite cluster's curvature, which varies inversely with the cluster radius. Finally, a critical radius is approximated.

Each model assumes a circular cluster with radius  $R(t)$  at time  $t$ , and writes the dynamics of the cluster radius as:

$$\partial R/\partial t = v^* - D/R \quad (1)$$

where  $v^*$  is the asymptotic velocity at which the invader advances as a planar wave (i.e. the velocity reached as time advances and  $R \rightarrow \infty$ , so that curvature become negligible) and  $D$  is the *effective* diffusion coefficient. The cluster's curvature is proportional to  $R^{-1}$ , so that both increased diffusion and a smaller radius reduce cluster expansion. When  $R = R_{\text{crit}}$ ,  $\partial R/\partial t = 0$ , so that  $R_{\text{crit}} = D/v^*$ . In the model of Lewis and Kareiva (1993),  $R_{\text{crit}}$  increases as either the diffusion coefficient  $D$  or the Allee effect increases, and decreases as the invader's intrinsic growth rate increases. Gandhi *et al.* (1999) give the same ratio for the critical radius, although the planar velocity in their two-species competition analysis depends on model-specific parameters. After we present our results, we comment on the applicability of the  $D/v^*$  approximation to the continuum reaction-diffusion equations that correspond to the details of our stochastic model of spatial competition.

## NUCLEATION AND THE CRITICAL RADIUS

We assume that an introduction produces a spatial aggregation of individual invaders, and that the initial dynamics is inherently stochastic. Local densities constrain the invader's propagation preemptively (Amarasekare, 2003; Shurin *et al.*, 2004; Tainaka *et al.*, 2004), so that competition for space drives cluster growth and decay. We have investigated invader–resident competition on a lattice (Korniss and Caraco, 2005; O'Malley *et al.*, 2005) by applying the physical theory for nucleation of spatial systems (Rikvold *et al.*, 1994; Ramos *et al.*, 1999; Kashchiev, 2000; Korniss *et al.*, 2001). The results link local propagation rates to global population dynamics, and indicate a critical cluster size for invader growth (O'Malley *et al.*, 2005, 2006a). That is, if an invader cluster attains the critical radius (grows to critical size), further expansion and decay have equal probability (Evans and Ray, 1994; ter Horst and Kashchiev, 2003); a nucleation 'event' occurs when a growing cluster reaches the critical radius. Smaller clusters are more likely to decay than grow, either due to competition from the resident or chance excess of invader mortality over propagation. Expansion is more likely than decay for clusters exceeding the critical size, and continued growth may allow the invader to exclude the resident species. Nucleation theory addresses invasion by either a single invader cluster or multiple clusters; the critical-radius concept applies in each mode. Korniss and Caraco (2005), O'Malley *et al.* (2005, 2006a), and Yasi *et al.* (2006) detail the application of nucleation theory to the evolutionary ecology of invasion dynamics.

### An individual-based stochastic model of preemptive competition

Consider an  $L \times L$  lattice with periodic boundary conditions; a lattice site represents the minimum level of local resources required to sustain a single organism. Hence, each site is either empty or occupied by a resident or an invader. The local occupation numbers at site  $\mathbf{x}$ ,  $n_i(\mathbf{x}) = 0, 1$ ;  $i = 1, 2$  represent the number of resident and invader individuals, respectively. Competition for space is preemptive (Amarasekare, 2003; Shurin *et al.*, 2004; Oborny *et al.*, 2005; Sintés *et al.*, 2005); an individual of either species may propagate clonally only if one or more of the  $\delta$  nearest-neighbouring sites is empty.

If a site is empty, introduction *or* clonal propagation from the surrounding neighbourhood can occur. The rate for introduction of an invader is  $\beta$ . The rate for colonization by species  $i$  occupying neighbouring sites is given by  $\alpha_i \eta_i(\mathbf{x})$ , where  $\alpha_i$  is the individual-level colonization rate and  $\eta_i(\mathbf{x}) = (1/\delta) \sum_{\mathbf{x}' \in \sigma(\mathbf{x})} n_i(\mathbf{x}')$  is the density of species  $i$  around site  $\mathbf{x}$ .  $\sigma(\mathbf{x})$  is the set of neighbours of site  $\mathbf{x}$ , and  $\delta = |\sigma(\mathbf{x})|$  is the size of this neighbourhood. If the site is occupied by an individual of species  $i$ , that individual dies at rate  $\mu_i$ . Summarizing the transition rates for an arbitrary site  $\mathbf{x}$ ,

$$0 \xrightarrow{\alpha_i \eta_i(\mathbf{x})} 1, \quad 0 \xrightarrow{\beta + \alpha_2 \eta_2(\mathbf{x})} 2, \quad 1 \xrightarrow{\mu_1} 0, \quad 2 \xrightarrow{\mu_2} 0, \quad (2)$$

where 0, 1, 2 indicate whether the site is empty, occupied by a resident or occupied by an invader, respectively. In our simulations below, we set  $\beta = 0$ ,  $\mu \equiv \mu_1 = \mu_2$ , select the size of an invader cluster, and ask if the cluster grows or decays.

### A deterministic, geometric approach to the critical radius

Our spatial competition model and, more generally, nucleation theory base their predictions on probabilistic growth and decline of densities. However, before turning to simulation of the individual-based stochastic spatial model, we develop a deterministic ‘competitive balance’ model for the geometry of local propagation to identify hypotheses to test with the spatial model.

Here, we assume continuous space and take both the invader cluster and the local colonization neighbourhood as circles. The environment is a finite two-dimensional space, where individuals of two species occur as events of a spatial point process. The  $\alpha_i$  are propagule-production rates, and the  $\mu_i$  ( $i = 1, 2$ ) are mortality rates per unit density (see definitions above). We assume that propagation rates are sufficiently large that either species, when alone, avoids extinction due to mortality. The invader possesses a competitive advantage:  $\alpha_2/\mu_2 > \alpha_1/\mu_1$ . In this paper, we restrict attention to the case where  $\mu \equiv \mu_1 = \mu_2$  (implying that  $\alpha_2 > \alpha_1$ ).

An invader cluster lies within  $C$ , a circle with radius  $R$ ;  $C$  is centred at the origin  $O$  (see Fig. 1). No residents occur within  $C$ , but individuals of the resident species surround  $C$ , at density  $\rho_1$ , a function of  $\alpha_1$  and  $\mu$ . The invading species may equilibrate stochastically within  $C$ , or, as an initial condition for small  $R$ , may take some arbitrary density on  $C$ . For either case, we represent the expected density of invaders within  $C$  by  $\rho_2$ . Competition constrains the total density of individuals per neighbourhood, defined below, to lie on  $[0, 1]$ . Therefore,  $0 \leq \rho_i \leq 1$ ;  $i = 1, 2$ .

Consider a location, designated  $k$ , on the perimeter of  $C$  (Fig. 1). Assume that species  $i$  has just dispersed an offspring to  $k$ , but we do not know whether  $i = 1$  or 2. Given the spatial constraint on propagation, and assuming that introduction from outside the environment occurs rarely (equivalently,  $\beta = 0$ ), only individuals occupying the colonization neighbourhood around  $k$  can place offspring there. Designate the colonization neighbourhood  $\delta_k$ , a circle with radius  $r$ , centred at location  $k$  (Fig. 1). The neighbourhood radius  $r$  represents the maximal directed distance over which an individual can disperse propagules. Both species occur on  $\delta_k$ , but the invader’s spatial clustering implies that the two species will occupy distinct areas within the neighbourhood  $\delta_k$ . The invader occurs on region  $\{C \cap \delta_k\}$ ; the resident occurs on region  $\delta_k \setminus \{C \cap \delta_k\}$ . Let  $m(2)$  represent the measure

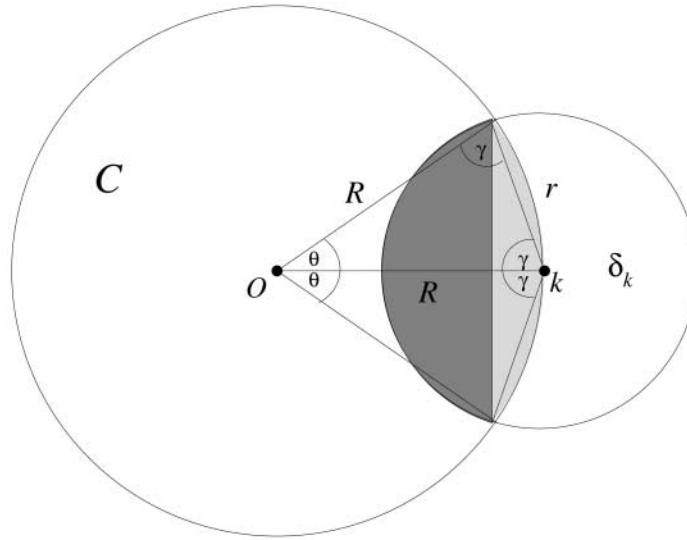


**Fig. 1.** Partitioning of the interaction neighbourhood.  $C$  is the invader cluster and  $\delta_k$  is the neighbourhood about site  $k$ . See text for details.

of region  $\{C \cap \delta_k\}$ , where species 2, the invader, occurs.  $m(1)$  is the measure of the region  $\delta_k \setminus \{C \cap \delta_k\}$ , where the resident, species 1, occurs. Then  $m(1) + m(2) = \pi r^2$ .

We represent the critical radius of the invader cluster by  $R_{crit}$ . Given that a newly ‘born’ individual has just appeared at  $k$ ,  $R = R_{crit}$  if that individual is equally likely to be a resident or an invader. Therefore, each species must have attempted to colonize site  $k$  at the same total probabilistic rate. So, we have ‘competitive balance’:

$$R = R_{crit} \Leftrightarrow m(1) \rho_1 \alpha_1 = m(2) \rho_2 \alpha_2 \tag{3}$$

Equivalently, invader-cluster size ( $\pi R^2$ ) reaches a critical size (ter Horst and Kashchiev, 2003) when  $R = R_{crit}$ . To analyse the critical radius, we first obtain the areas  $m(i)$  as functions of  $R$  and  $r$ , using elementary geometrical considerations. Then, invoking the simple balance assumption of equation (3), we find  $R_{crit}$  as a function of  $\alpha_1, \alpha_2, \mu, r$ . The ‘quasi’-equilibrium densities  $\rho_1$  and  $\rho_2$  depend on underlying model parameters  $\alpha_1, \alpha_2$ , and  $\mu$ . Given values of these parameters, we can evaluate the densities using the stochastic model’s mean-field or pair approximation (see Appendix 2).

### Partitioning the interaction neighbourhood

We generally expect that  $r < 2R$ . If  $r \geq 2R$ , the invader cluster lies entirely within the colonization neighbourhood and, trivially,  $m(2) = \pi R^2$ . Then, for the resident,  $m(1) = \pi(r^2 - R^2)$ . Here, we obtain  $m(2)$  for the relevant case,  $r < 2R$ , by finding the area common to partially overlapping circles.

First, we determine the area, inside the colonization neighbourhood, corresponding to the invader-region  $\{C \cap \delta_k\}$ . As can be seen in Fig. 1, this is the overlap of the two circular regions; one has radius  $R$  and the other has radius  $r$ . We divide this region of overlap into two segments: a circular segment with radius  $R$  and opening angle  $2\theta$  (lighter shading in

Fig. 1), and another circular segment with radius  $r$  and opening angle  $2\gamma$  (darker shading in Fig. 1). Clearly, the two angles are related by  $\theta + 2\gamma = \pi$ , and furthermore,  $r/(2R) = \cos(\gamma) = \sin(\theta/2)$ . Elementary geometric identities yield the areas of the circular segments as  $\frac{R^2}{2} [2\theta - \sin(2\theta)]$  and  $\frac{r^2}{2} [2\gamma - \sin(2\gamma)]$ , respectively. Combining areas of these segments yields the area of  $\{C \cap \delta_k\}$ . Using standard trigonometric identities, we find:

$$\begin{aligned}
 m(2) &= \frac{R^2}{2} [2\theta - 2\sin(\theta)\cos(\theta)] + \frac{r^2}{2} [\pi - \theta - \sin(\pi - \theta)] \\
 &= 2R^2 \arcsin\left(\frac{r}{2R}\right) - Rr\sqrt{1 - \left(\frac{r}{2R}\right)^2} \left(1 - \frac{r^2}{2R^2}\right) + \\
 &\quad \pi r^2/2 - r^2 \arcsin\left(\frac{r}{2R}\right) - r^3/2R\sqrt{1 - \left(\frac{r}{2R}\right)^2} \\
 &= \pi r^2/2 + 2R^2\left(1 - \frac{r^2}{2R^2}\right) \arcsin\left(\frac{r}{2R}\right) - Rr\sqrt{1 - \left(\frac{r}{2R}\right)^2}
 \end{aligned} \tag{4}$$

and, trivially,  $m(1) = \pi r^2 - m(2)$ . In general, by substituting equation (4) into equation (3), one can obtain the critical radius numerically for any given set of parameters, so that  $R_{\text{crit}} = R_{\text{crit}}(\alpha_1, \alpha_2, \mu, r)$ . Appendix 1 describes the approximate behaviour of  $m(2)$  for  $r/R \ll 1$ , which can be used to obtain  $R_{\text{crit}}$  in the  $(\alpha_2 - \alpha_1) \rightarrow 0$  limit (see next section).

### CRITICAL RADIUS AND ECOLOGICAL INVASION

Before quantifying the critical radius' dependence on propagation and mortality rates, we list intuitive, qualitative predictions about cluster-growth probabilities. From equation (3) we have  $m(2) = m(1)(\rho_1 \alpha_1/\rho_2 \alpha_2)$  when  $R = R_{\text{crit}}$ , i.e. when cluster growth and decay have equal probability. Since  $m(1) + m(2) = \pi r^2$ ,

$$m(2) = \pi r^2 \left( \rho_1 \alpha_1 / [\rho_1 \alpha_1 + \rho_2 \alpha_2] \right) \tag{5}$$

Any increase in  $m(2)$  required to maintain equality of the two species' expected colonization rates, as expressed in equation (3), implies an increase in  $R_{\text{crit}}$ . Simple consequences of equation (5) include the following:

- $\partial R_{\text{crit}}/\partial \alpha_1 > 0$ . Resident density,  $\rho_1$ , increases with its propagation rate  $\alpha_1$ . To maintain criticality,  $m(2)$  must then increase with  $\alpha_1$ ; the invader cluster must be larger if the resident's total rate of propagule production per unit area increases.
- $\partial R_{\text{crit}}/\partial \alpha_2 < 0$ . The invader cluster need not be as large if the individual rate of propagule production, hence production per unit area, increases.

These two predictions imply that  $\partial R_{\text{crit}}/\partial(\alpha_2 - \alpha_1) < 0$  (Appendix 2 provides some detail). Generally, we expect that the critical radius scales as  $(\alpha_2 - \alpha_1)^{-\phi}$ , where  $\phi > 0$ , as  $(\alpha_2 - \alpha_1) \rightarrow 0$ ; that is,  $R_{\text{crit}}$  grows exceedingly large as  $\alpha_1 \rightarrow \alpha_2$  (Evans and Ray, 1994; O'Malley *et al.*, 2006a).

- $\partial R_{\text{crit}}/\partial \delta_k > 0$ . As the size of the colonization neighbourhood  $\delta_k$  increases (equivalently,  $r$  increases), more resident individuals attempt to colonize space at the periphery of the invader cluster. To counter this numerical effect,  $R_{\text{crit}}$  must increase, so that the curvature of the invader cluster declines.
- $\partial R_{\text{crit}}/\partial \mu < 0$ . Mortality rates can influence  $R_{\text{crit}}$  through the densities  $\rho_i$ , which in turn affect total propagule production. Appendix 2 evaluates two equilibrium models for the  $\rho_i$ , based respectively on a mean-field approximation and a pair approximation to the dynamics associated with our individual-based cluster-growth model (O'Malley *et al.*, 2006a). For the case we study in this paper ( $\mu = \mu_1 = \mu_2$ ), each analysis in Appendix 2 finds that increased mortality permits the invader to advance more readily.

The last prediction has a simple basis. For convenience, suppose the two species take mean-field densities in their respective regions. Then  $\rho_2 = 1 - (\mu/\alpha_2)$  for the invader on  $\{C \cap \delta_k\}$ , and  $\rho_1 = 1 - (\mu/\alpha_1)$  for the resident on  $\delta_k \setminus \{C \cap \delta_k\}$ . Since  $\alpha_1 < \alpha_2$ , an increase in mortality rate  $\mu$  reduces the density of the resident faster than it reduces the density of the invader. Hence the invader cluster can grow more readily, and the critical radius will decline. However, our geometric model of the critical radius is deterministic and, as stressed above, invasion dynamics is inherently stochastic. For smaller invader clusters, an increase in mortality might increase the likelihood of chance extinction sufficiently to more than offset the greater availability of open sites at the cluster's periphery (e.g. Caraco *et al.*, 1998).

These properties of the geometric model's  $R_{\text{crit}}$  suggest predictions for cluster-growth probabilities. Consider an invader cluster of radius  $R$ .  $P_s(R)$  represents the probability that the cluster succeeds – that is, grows and generates an invasion. The cluster decays with probability  $1 - P_s(R)$ . For any given radius  $R$ ,  $P_s(R)$  varies inversely with  $R_{\text{crit}}$ , since factors inhibiting invasion should increase the critical radius. Given these assumptions, the geometric model implies that the probability a cluster with radius  $R$  generates a successful introduction varies inversely with the resident's propagation rate  $\alpha_1$ , varies directly with the invader propagation rate  $\alpha_2$ , varies inversely with colonization-neighbourhood size  $\delta_k$ , and increases with the common mortality rate  $\mu$ .

To quantify these predictions, we calculated the critical radius according to the geometric partitioning of the interaction neighbourhood, and separately addressed cluster-success probabilities by simulating the stochastic individual-based model. The first analysis substitutes the area of  $\delta_k$  occupied by the invader, equation (4), into equation (3) and solves for  $R_{\text{crit}}$  as explained above. For the densities, we used values given by pair approximation, equation (A2.4) of Appendix 2. We repeated the calculation using mean-field densities of Appendix 2 and obtained very similar values for  $R_{\text{crit}}$ .

Figure 2a plots the geometric model's critical radius against the difference in propagation rates ( $\alpha_2 - \alpha_1$ ), for  $\alpha_2 = 0.7$  and  $0.5 \leq \alpha_1 \leq 0.68$ . Given our parameter values,  $R_{\text{crit}}$  increased with an increase in neighbourhood size  $\delta_k$ , and decreased as the common mortality rate  $\mu$  increased. Not surprisingly,  $R_{\text{crit}}$  decreased as  $(\alpha_2 - \alpha_1)$  increased. More specifically, the logarithmic scaling of Fig. 2 shows that  $R_{\text{crit}} \sim (\alpha_2 - \alpha_1)^{-\phi}$ , where  $1.06 \leq \phi \leq 1.12$  (least squares estimates). Hence  $(\alpha_2 - \alpha_1) R_{\text{crit}} \approx 1$  in these calculations, when the  $\rho_i$  have either the pair-approximation or mean-field equilibrium values. This scaling need not hold if the densities  $\rho_i$  are functionally decoupled from the  $\alpha_i$  (results not shown).

Figure 2b plots corresponding results as  $\alpha_1 \rightarrow \alpha_2$ ;  $\alpha_2 = 0.7$  and  $0.69 \leq \alpha_1 \leq 0.6995$ . A larger neighbourhood increased  $R_{\text{crit}}$ , and a greater mortality rate decreased  $R_{\text{crit}}$ . For these

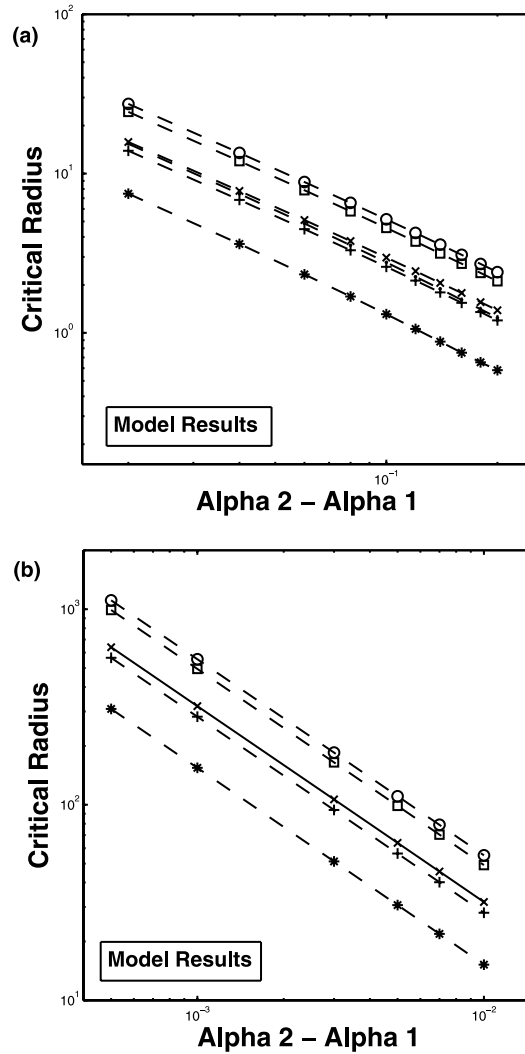


**Fig. 2.** (a) Critical radius in deterministic ('competitive balance') model of cluster geometry:  $0.5 \leq \alpha_1 \leq 0.68$ . Geometric model of critical radius, with each species' density set at its respective pair-approximation equilibrium (see Appendix 2).  $R_{\text{crit}} \sim (\alpha_2 - \alpha_1)^{-\phi}$ , where  $1.06 \leq \phi \leq 1.12$ . Symbols are  $\circ$  ( $\delta = 12, \mu = 0.03$ );  $\square$  ( $\delta = 12, \mu = 0.1$ );  $\times$  ( $\delta = 4, \mu = 0.03$ );  $\bullet$  ( $\delta = 12, \mu = 0.3$ );  $+$  ( $\delta = 4, \mu = 0.1$ );  $\star$  ( $\delta = 4, \mu = 0.3$ ). Deterministic model's critical radius increases as neighbourhood size increases, and decreases as mortality rate increases. (b) Critical radius in deterministic model of cluster geometry:  $0.69 \leq \alpha_1 \leq 0.6995$ . Geometric model of critical radius, with each species' density set at its respective pair-approximation equilibrium (see Appendix 2).  $R_{\text{crit}} \sim (\alpha_2 - \alpha_1)^{-\phi}$ , where  $1.0 \leq \phi \leq 1.01$ , so that  $(\alpha_2 - \alpha_1)R_{\text{crit}} \approx 1$ . Symbols are  $\circ$  ( $\delta = 12, \mu = 0.03$ );  $\square$  ( $\delta = 12, \mu = 0.1$ );  $\times$  ( $\delta = 4, \mu = 0.03$ , and  $\delta = 12, \mu = 0.3$ );  $+$  ( $\delta = 4, \mu = 0.1$ );  $\star$  ( $\delta = 4, \mu = 0.3$ ). Solid line connects values for ( $\delta = 4, \mu = 0.03$ ) and ( $\delta = 12, \mu = 0.3$ ), which fall together given the ordinate's scaling. Qualitative results are the same as Fig. 2a.

parameter values,  $R_{\text{crit}} \sim (\alpha_2 - \alpha_1)^{-\phi}$ , where  $1.0 \leq \phi \leq 1.01$  (least squares estimates), so that again  $(\alpha_2 - \alpha_1) R_{\text{crit}} \approx 1$ .

To gain further insight into the basis of this power law, we obtained the approximate behaviour of  $R_{\text{crit}}$  as  $(\alpha_2 - \alpha_1) \rightarrow 0$ . Since neighbourhood size ( $r$ ) is fixed,  $r/R_{\text{crit}} \ll 1$  in this limit, and we then can employ the approximate behaviour of the  $m(i)$  (Appendix 1) and the mean-field approximation for the densities of the two species (Appendix 2). Substituting mean-field equilibrium densities into equation (5), we have at the critical radius:  $m(1)(\alpha_1 - \mu) = m(2)(\alpha_2 - \mu)$ . From Appendix 1,

$$m(1,2) = \pi r^2 / 2 \left( 1 \pm 2 / 3\pi [r/R_{\text{crit}}] \right)$$

where the + and - signs correspond to  $m(1)$  and  $m(2)$ , respectively. Inserting these expressions into the condition for the critical radius yields, to leading order as  $(\alpha_2 - \alpha_1) \rightarrow 0$ , the approximation for  $R_{\text{crit}}$ :

$$R_{\text{crit}} \approx \frac{2}{3\pi} \frac{\alpha_1 + \alpha_2 - 2\mu}{\alpha_2 - \alpha_1} r \approx \frac{4}{3\pi} \frac{\alpha_2 - \mu}{\alpha_2 - \alpha_1} r \tag{6}$$

Thus, in the asymptotic ( $\alpha_1 \rightarrow \alpha_2$ ) limit, the geometric competitive-balance model yields  $R_{\text{crit}} \sim (\alpha_2 - \alpha_1)^{-1}$ , in agreement with the complete numerical solution of equation (4) for small differences in propagation rates, as demonstrated by the results shown in Fig. 2b.

### SIMULATION RESULTS FOR THE INDIVIDUAL-BASED SPATIAL MODEL

Employing the local rates defined earlier, we implemented dynamic Monte Carlo simulations on a  $10^3 \times 10^3$  lattice. The time unit was one Monte Carlo step per site, during which  $10^6$  sites were chosen randomly, and updated probabilistically according to our spatial model of ecological invasion. These procedures mimic the model's continuous-time dynamics (Korniss *et al.*, 1999). Throughout, we fixed  $\alpha_2 = 0.7$ . We chose six values for  $\alpha_1$  on [0.69, 0.6995] and simulated three mortality rates,  $\mu = 0.03, 0.1, \text{ and } 0.3$ .

We initialized the lattice with each site occupied by a resident. We ran the simulation for 50 time steps, during which the resident's global density rapidly decayed to its single-species equilibrium. We then set the simulation clock to  $t = 0$  and placed a single invader cluster on the lattice, with radius  $R(0)$ ; the initial number of invaders was proportional to  $[R(0)]^2$ . We simulated the spatial dynamics until  $t = 20,000$ , unless the invader first declined to extinction. We recorded a successful introduction only if the perimeter of the cluster expanded, and noted global densities of the invader and resident at the final time. For each parameter combination, we simulated invader-introduction 100 times. We cannot expect critical radii in the continuous-space geometric model to predict quantitative properties of the discrete-space lattice model. Rather, we asked if patterns suggested by the deterministic model of critical-radius geometry held up when clusters grow and decline probabilistically on a lattice.

Figure 3a plots the proportion of species-2 clusters that successfully invaded the resident (species 1) as a function of the invader cluster's initial radius  $R(0)$ . We set  $\delta_k = 4$  and  $\mu = 0.3$  in these simulations, and show results for six values of  $\alpha_1$ . As  $\alpha_1$  increases, the probability of cluster growth decreases for any  $R(0)$ , and  $R_{\text{crit}}$  increases.

The figure's logarithmic scaling of  $R(0)$  reveals sigmoid dependence of  $P_s$  on the initial cluster's radius. Let  $x = \log[R(0)]$ , and let  $P_s(x)$  represent the probability an introduction

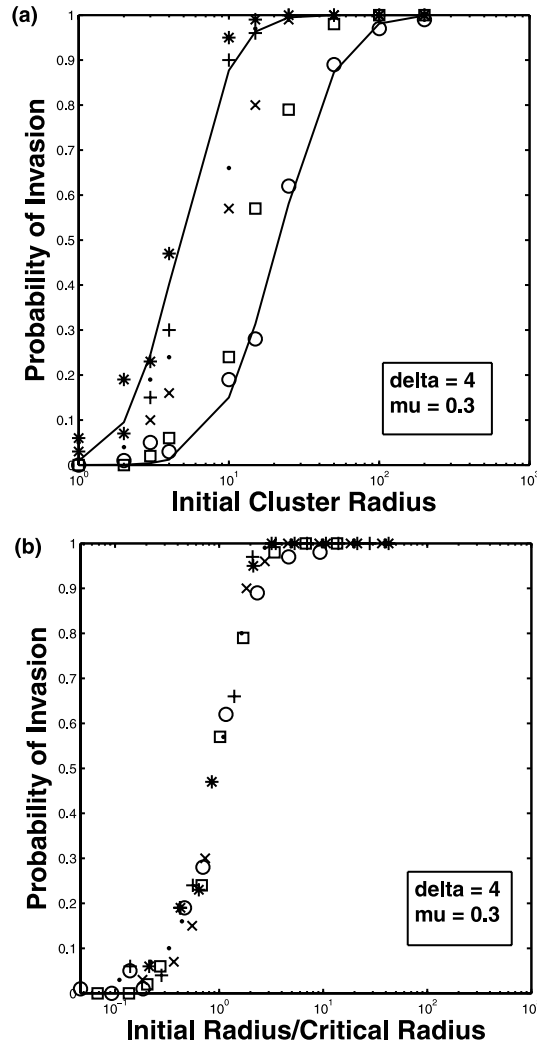


**Fig. 3.** (a) Probability of cluster growth; simulations of stochastic individual-based model with  $\delta = 4$  and  $\mu = 0.3$ .  $\alpha_2 = 0.7$ ; values for  $\alpha_1$  are 0.69 (\*), 0.693 (+), 0.695 (●), 0.697 (×), 0.699 (□), and 0.6995 (○). Solid lines show piecewise approximation to  $P_s(x) \approx (1/2)[1 + \text{erf}(\xi[x - x^*])]$  for  $\alpha_1 = 0.69$  ( $\xi = 2.5$ ) at left, and  $\alpha_1 = 0.6995$  ( $\xi = 2.2$ ) at right (see explanation in text). Invasion probability increases with  $(\alpha_2 - \alpha_1)$ ; at  $R_{\text{crit}}$ , invasion probability = 0.5. (b) Data collapse. Dividing each initial radius by the critical radius (for associated value of  $\alpha_1$ ) shows the basic relationship for which plots in Fig. 3a are examples.

with cluster radius  $10^x$  succeeds. At the critical radius, cluster growth and decay (the introduction's success or failure) are equally probable. If  $x^* = \log[R_{\text{crit}}]$ , then  $P_s(x^*) = 1/2$ . Following an analysis of cluster size by ter Horst and Kashchiev (2003), we can approximate  $P_s(x)$  using an error function:

$$P_s(x) \approx (1/2)[1 + \text{erf}(\xi[x - x^*])], \tag{7}$$

where

$$\operatorname{erf}(z) = \frac{2}{\pi^{1/2}} \int_0^z \exp[-s^2] ds,$$

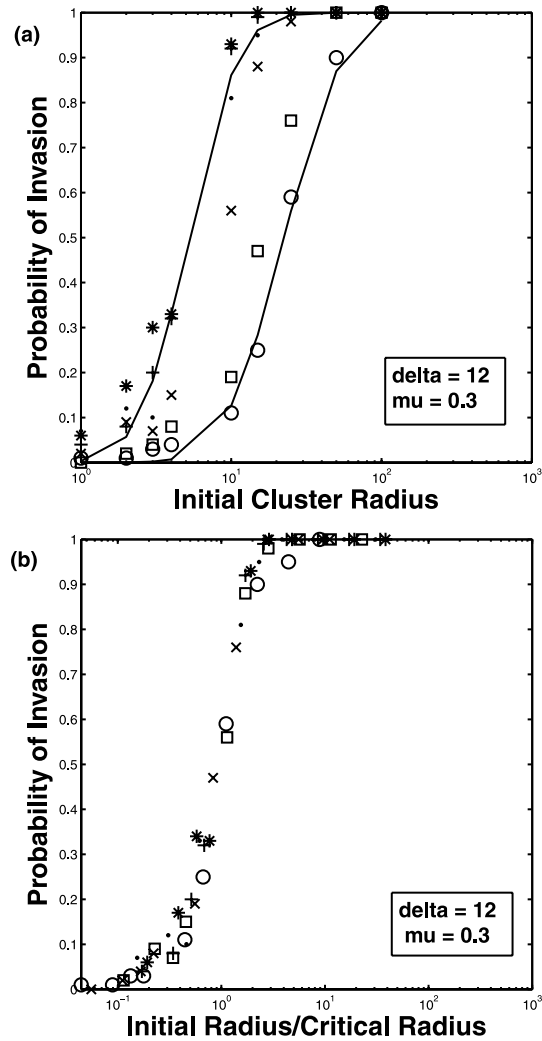
twice the integral of a normal density, and  $\xi > 0$ . From simulation results we read  $x^*$  by eye, and adjusted  $\xi$  numerically for the  $P_s$  values associated with each level of  $\alpha_1$ . Figure 3a shows that expression (7) approximates the simulation results fairly well. Since  $[x - x^*]$  in expression (7) is  $\log[R(0)/R_{\text{crit}}]$ , Fig. 3b plots invasion probability against  $R(0)/R_{\text{crit}}$ . The simulation data collapse nicely after scaling cluster radii by the critical value for each level of  $\alpha_1$ .

Figure 4a plots the chance that introduction succeeds against initial cluster radius for various levels of  $\alpha_1$  when  $\delta_k = 12$  and  $\mu = 0.3$ . Comparing Figs. 3a and 4a suggests that this increase in neighbourhood size had no consistent effect on the probability of cluster growth, contrary to predictions of the geometric model (Figs. 2a, b). Expression (7) again approximates the simulation results reasonably well. Figure 4b shows the clarifying data-collapse across levels of  $\alpha_1$  when each initial cluster radius is scaled by the critical radius.

Figure 5a plots the chance that introduction succeeds against initial cluster radius for various levels of  $\alpha_1$  when  $\delta_k = 4$  and  $\mu = 0.03$ . Comparing Figs. 3a and 5a indicates that the mortality-rate difference alters invasion probabilities and the critical radius. The comparison indicates that, for *larger* initial clusters and larger values of  $\alpha_1$ , invasion probabilities are greater at higher  $\mu$ . However, for *smaller* initial clusters, invasion probabilities are slightly smaller when mortality is greater; the effect again is clear for larger values of  $\alpha_1$ . Interaction of these effects results in a larger critical radius, for small differences in propagation rates, at the higher mortality rate. An increase in the critical radius and any decrease in cluster-growth probabilities induced by increasing the mortality rate (from 0.03 to 0.3) contradict the deterministic predictions. Figure 5b shows the cluster-growth probabilities when the initial radius is rescaled by the critical radius. Scaling achieves data collapse when  $0.01 \geq (\alpha_2 - \alpha_1) \geq 0.003$ , but the data are more variable for the two largest values of  $\alpha_1$ . For some of these simulations, 20,000 time steps produced no invader advance (hence introduction failed by our conservative definition), but the invader cluster remained far from extinction. As the two species become more similar, the time to competitive exclusion should increase rapidly (Gandhi *et al.*, 1999).

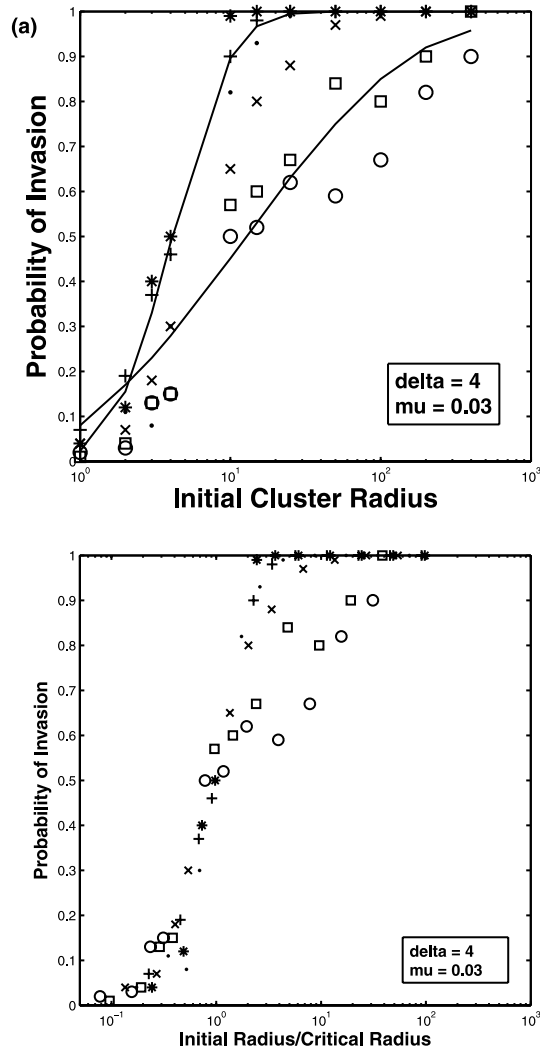
Figure 6 shows estimates (i.e. read from plots of  $P_s$ ) of the critical radius from simulations against the difference in propagation rates ( $\alpha_2 - \alpha_1$ ). Although our data have somewhat limited range, as a guide to a comparison with the results of the deterministic model (where  $R_{\text{crit}} \sim (\alpha_2 - \alpha_1)^{-\phi}$  with  $\phi \approx 1$ ), we plotted a line with a slope of  $-1/2$ . Our results clearly indicate that, if there is a power-law dependence, the scaling behaviour of the critical radius is governed by an exponent not greater than  $\phi = 1/2$  for the stochastic individual-based spatial model, in strong contrast with the result of the deterministic approximation.

Figure 6 also indicates that for sufficiently large ( $\alpha_2 - \alpha_1$ ), the critical radius varies little with either  $\delta_k$  or  $\mu$ ; a cluster of approximately 60 individuals (a radius of 4.4) is as likely to grow as decline. However, as  $\alpha_1 \rightarrow \alpha_2$ , the critical radius increases as mortality increases, and the scaling exponent  $\phi$  appears to increase towards  $1/2$ . Any advantage in relative density the invader might gain by an increase in the common mortality rate (see above) is likely



**Fig. 4.** (a) Probability of cluster growth; simulations of stochastic individual-based model with  $\delta = 12$  and  $\mu = 0.3$ .  $\alpha_2 = 0.7$ ; values for  $\alpha_1$  are 0.69 (\*), 0.693 (+), 0.695 (●), 0.697 (x), 0.699 (□), and 0.6995 (○). Solid lines show piecewise approximation to  $P_s(x) \approx (1/2)[1 + \text{erf}(\xi[x - x^*])]$  for  $\alpha_1 = 0.69$  ( $\xi = 2.7$ ) at left, and  $\alpha_1 = 0.6995$  ( $\xi = 2.3$ ) at right (see text). At  $R_{crit}$ , invasion probability = 0.5. (b) Data collapse as in Fig. 3b.

offset by an increase in chance extinction of smaller clusters. To support this interpretation, we plot the average time to extinction for those invader clusters that fail to advance. Figure 7a shows extinction times, as a function of initial cluster radius, for  $\delta_k = 4$ ; Fig. 7b plots corresponding means for  $\delta = 12$ . The figures indicate the relative rapidity at which small clusters disappear at the higher level of mortality (O'Malley *et al.*, 2006a).



**Fig. 5.** (a) Probability of cluster growth; simulations of stochastic, individual-based model with  $\delta = 4$  and  $\mu = 0.03$ .  $\alpha_2 = 0.7$ ; values for  $\alpha_1$  are 0.69 (\*), 0.693 (+), 0.695 (●), 0.697 (x), 0.699 (□), and 0.6995 (○). Solid lines show piecewise approximation to  $P_s(x) \approx (1/2)[1 + \text{erf}(\zeta[x - x^*])]$  for  $\alpha_1 = 0.69$  ( $\zeta = 2.3$ ) at left, and  $\alpha_1 = 0.6995$  ( $\zeta = 0.82$ ) at right (see text). At  $R_{\text{crit}}$ , invasion probability = 0.5. (b) Data collapse as in Fig. 3b; results good for four lowest values of  $\alpha_1$ .

### NOTES ON THE REACTION-DIFFUSION APPROXIMATION

For the local rates defining our stochastic spatial model, one can systematically derive a deterministic partial differential equation (PDE) (see O'Malley *et al.*, 2006b, in press). Taking the exact Master equation for the many-particle stochastic process given by those rates on a lattice, neglecting correlations between densities at different sites (McKane and Newman, 2004), and taking the naïve continuum limit, one obtains the equations of motions (O'Malley *et al.*, 2006b, in press):

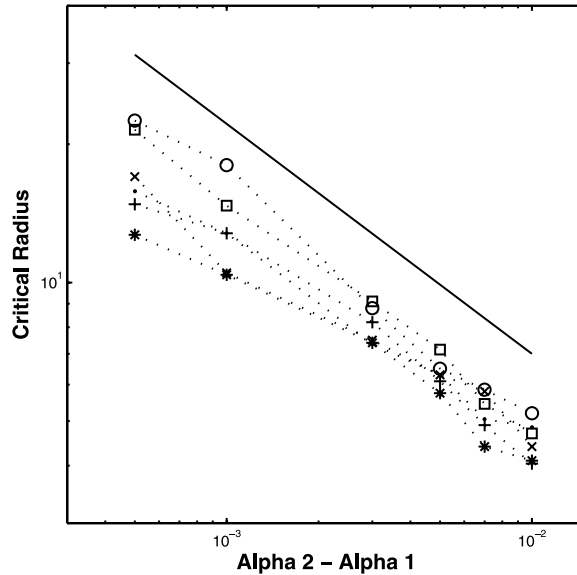


**Fig. 6.** Critical radius from simulations. Values read by eye from simulation plots of invasion probability against initial cluster radius.  $\alpha_2 = 0.7$  throughout. Symbols are  $\circ$  ( $\delta = 12, \mu = 0.3$ ),  $\square$  ( $\delta = 4, \mu = 0.3$ ),  $\times$  ( $\delta = 4, \mu = 0.1$ ),  $\bullet$  ( $\delta = 12, \mu = 0.1$ ),  $+$  ( $\delta = 12, \mu = 0.03$ ), and  $*$  ( $\delta = 4, \mu = 0.03$ ). Since the values were read by eye, we simulated the model using plotted radii; mean proportion of successful invasion was  $0.504 (\pm 0.025, 95\% \text{ confidence interval})$ , not different than 0.5. The bold solid line with a slope of  $-1/2$  serves as a guide to compare the results with the behaviour of the deterministic model (which predicts a slope of  $-1$ ).

$$\partial \rho_i / \partial t = (\alpha_i / 4)(1 - \rho_1 - \rho_2) \nabla^2 \rho_i + \alpha_i(1 - \rho_1 - \rho_2) \rho_i - \mu \rho_i; \quad i = 1, 2 \quad (8)$$

where  $\nabla^2$  is the Laplacian. (Note that the diffusive term in the present model is *not* the result of individual mobility, but a consequence of local vegetative propagation.) A simple analysis of the above equations (for  $\mu < \alpha_1 < \alpha_2$ ) implies that starting from a sufficiently sharp initial interface separating the competing species, invaders (species 2) propagate into an *unstable phase*, dominated by residents (species 1). This phenomenon has generated a vast literature since the original papers by Fisher (1937) and Kolmogorov *et al.* (1937). At the level of the above deterministic continuum PDE, the front is ‘pulled’ by the *leading edge* into the unstable phase (Ebert and van Saarloos, 2000; Murray, 2002; van Saarloos, 2003). For circular fronts in two dimensions, however, the curvature correction to the radial velocity in equation (1),  $[-D/R(t) \sim O(1/t)]$ , is comparable to the temporal correction (or rate of convergence) to the asymptotic velocity of linear fronts, also of  $O(1/t)$  (Ebert and van Saarloos, 2000; van Saarloos, 2003). Hence, for pulled fronts, one cannot use equation (1) to determine the critical radius in a self-consistent fashion. The scenario is drastically different for ‘pushed’ fronts, or propagation into (meta)stable states [as is the case in the Lewis and Kareiva (1993) model with an Allee effect], where convergence to the asymptotic velocity is exponentially fast, so that equation (1) indeed represents the asymptotic leading order correction to the velocity of a circular front (Ebert and van Saarloos, 2000; van Saarloos, 2003).

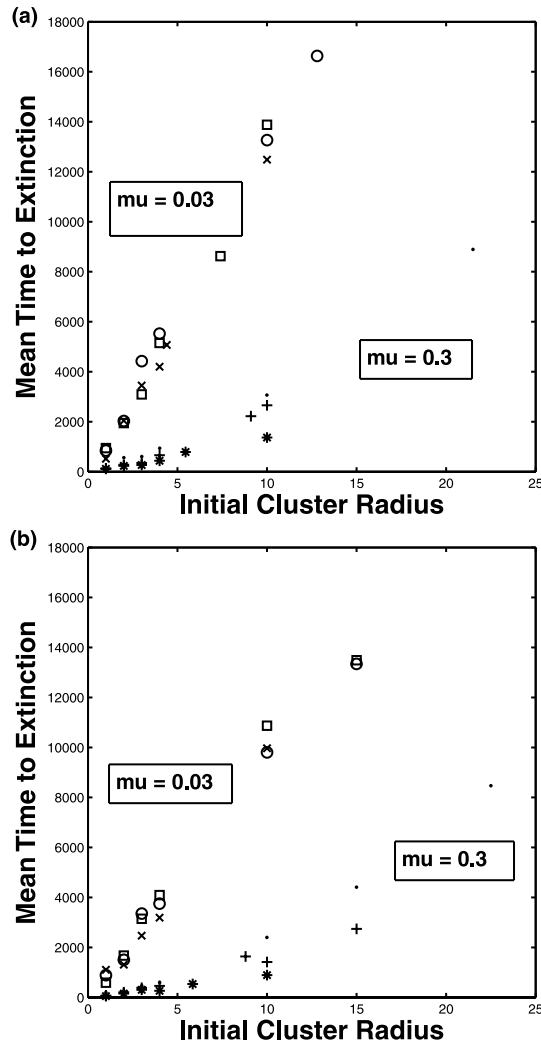


**Fig. 7.** (a) Mean time to extinction in simulation for failed invader clusters;  $\delta = 4$ . For  $\mu = 0.03$ ,  $\alpha_1 = 0.693$  ( $\times$ ),  $0.697$  ( $\square$ ), and  $0.6995$  ( $\circ$ ). For  $\mu = 0.3$ ,  $\alpha_1 = 0.693$  ( $*$ ),  $0.697$  ( $+$ ), and  $0.6995$  ( $\bullet$ ).  $\alpha_2 = 0.7$ . Values for  $\mu = 0.1$  intermediate to results plotted. (b) Mean time to extinction in the simulation for failed invader clusters;  $\delta = 12$ . Symbols as in (a). Small clusters are subject to relatively rapid, chance extinction at higher mortality rate.

### DISCUSSION

Our deterministic model of the critical-cluster radius, while it appreciates geometric aspects of preemptive competition between species, failed to predict effects of varying the common mortality rate observed in simulation of the stochastic invasion process. Furthermore, our individual-based simulation results indicate that the critical radius scales with the difference in propagation rates as  $R_{\text{crit}} \sim (\alpha_2 - \alpha_1)^{-\phi}$  with  $\phi \leq 1/2$ , in strong contrast with the deterministic geometrical approximation ( $\phi \approx 1$ ).

Our simulations suggest that an increase in mortality can increase the chance of invasion for large clusters, but can decrease the chance of invasion for small clusters. Our model assumes preemptive competition, so that a site occupied by a resident becomes available for colonization by the invader only through the resident's mortality. We suppose increased mortality more often drives small invader clusters extinct through chance events (Kot *et al.*, 2004). But larger clusters are, of course, safer from chance extinction. Increased mortality more often opens resident-occupied sites around the periphery of a larger cluster, and can consequently increase the chance of further expansion by the competitively superior invader (Korniss and Caraco, 2005).

The concept of a critical radius for invasive growth suggests a framework for organizing understanding of the apparent uncertainty associated with the outcome of any given species' introduction (Veltman *et al.*, 1996; Simberloff, 2000), at least for species that aggregate as a consequence of local dispersal. The outcome of an invader's initial introduction and, more generally, the dynamics of rarity can be inherently stochastic, discrete, and spatially structured (Durrett and Levin, 1994; Ellner *et al.*, 1998; Lewis and Pacala, 2000; Korniss and Caraco, 2005). Nucleation theory, applied to the invasion problem, appreciates each of these fundamental properties (O'Malley *et al.*, 2005, in press). More importantly, nucleation theory offers a general framework for predicting global dynamics of invader and resident species, as a function of demographic rates at the level of individuals (O'Malley *et al.*, 2006a, 2006b).

#### ACKNOWLEDGEMENTS

The material presented is based on work supported by the National Science Foundation under Grant No. 0342689. We thank J. de Koning for help with computing, and appreciate discussion with L. O'Malley, B. Kozma, and Z. Racz.

#### REFERENCES

- Amarasekare, P. 2003. Competitive coexistence in spatially structured environments: a synthesis. *Ecol. Lett.*, **6**: 1109–1122.
- Andow, D.A., Kareiva, P.M., Levin, S.A. and Okubo, A. 1990. Spread of invading organisms. *Land. Ecol.*, **4**: 177–188.
- Bauch, C. and Rand, D.A. 2000. A moment closure model for sexually transmitted disease transmission through a concurrent partnership network. *Proc. R. Soc. Lond. B*, **267**: 2019–2027.
- Butin, E., Porter, A.H. and Elkinton, J. 2005. Adaptation during biological invasions and the case of *Adelges tsugae*. *Evol. Ecol. Res.*, **6**: 887–900.
- Caraco, T., Duryea, M., Gardner, G., Maniatty, W. and Szymanski, B. 1998. Host spatial heterogeneity and extinction of an SIS epidemic. *J. Theor. Biol.*, **192**: 351–362.
- Caraco, T., Glavanakov, S., Chen, G., Flaherty, J.E., Ohsumi, T.K. and Szymanski, B.K. 2002. Stage-structured infection transmission and a spatial epidemic: a model for Lyme disease. *Am. Nat.*, **160**: 348–359.
- Caraco, T., Glavanakov, S., Li, S., Maniatty, W. and Szymanski, B.K. 2006. Spatially structured superinfection and the evolution of disease virulence. *Theor. Popul. Biol.*, **69**: 367–384.
- Cassey, P. 2003. A comparative analysis of the relative success of introduced land birds on islands. *Evol. Ecol. Res.*, **5**: 1011–1021.
- Dickman, R. 1986. Kinetic phase transitions in a surface-reaction model: mean-field theory. *Phys. Rev. A*, **34**: 4246–4250.
- Durrett, R. and Levin, S.A. 1994. The importance of being discrete (and spatial). *Theor. Popul. Biol.*, **46**: 363–394.

- Duryea, M., Caraco, T., Gardner, G., Maniatty, W. and Szymanski, B.K. 1999. Population dispersion and equilibrium infection frequency in a spatial epidemic. *Physica D*, **132**: 511–519.
- Dwyer, G. and Elkinton, J.S. 1995. Host dispersal and the spatial spread of insect populations. *Ecology*, **76**: 1261–1275.
- Ebert, U. and van Saarloos, W. 2000. Front propagation into unstable states: universal algebraic convergence towards uniformly translating pulled fronts. *Physica D*, **146**: 1–99.
- Ellner, S.P., Sasaki, A., Haraguchi, Y. and Matsuda, H. 1998. Speed of invasion in lattice population models: pair-edge approximation. *J. Math. Biol.*, **36**: 469–484.
- Evans, J.W. and Ray, T.R. 1994. Interface propagation and nucleation phenomena for discontinuous poisoning transitions in surface-reaction models. *Phys. Rev. E*, **50**: 4302–4314.
- Ferriere, R. and Gatto, M. 1995. Lyapunov exponents and the mathematics of invasion in oscillatory or chaotic populations. *Theor. Pop. Biol.*, **48**: 126–171.
- Fisher, R.A. 1937. The wave of advance of advantageous genes. *Ann. Eugenics*, **7**: 355–369.
- Frantzen, J. and van den Bosch, F. 2000. Spread of organisms: can travelling and dispersive waves be distinguished? *Basic Appl. Ecol.*, **1**: 83–91.
- Gandhi, A., Levin, S. and Orszag, S. 1999. Nucleation and relaxation from meta-stability in spatial ecological models. *J. Theor. Biol.*, **200**: 121–146.
- Kashchiev, D. 2000. *Nucleation: Basic Theory with Applications*. Oxford: Butterworth-Heinemann.
- Kolmogorov, A.N., Petrovsky, I. and Piscounoff, N. 1937. Study of the diffusion equation with growth of the quantity of matter and its application to a biology problem. *Moscow Univ. Bull. Math.*, **1**: 1–25.
- Korniss, G. and Caraco, T. 2005. Spatial dynamics of invasion: the geometry of introduced species. *J. Theor. Biol.*, **233**: 137–150.
- Korniss, G., Novotny, M.A. and Rikvold, P.A. 1999. Parallelization of a dynamic Monte Carlo algorithm: a partially rejection-free conservative approach. *J. Computational Phys.*, **153**: 488–494.
- Korniss, G., White, C.J., Rikvold, P.A. and Novotny, M.A. 2001. Dynamic phase transition, universality, and finite-size scaling in the two dimensional kinetic Ising model in an oscillating field. *Phys. Rev. E*, **63**: 016120 (15 pages).
- Kot, M., Lewis, M.A. and van den Driessche, P. 1996. Dispersal data and the spread of invading organisms. *Ecology*, **77**: 2027–2042.
- Kot, M., Medlock, J., Reluga, T. and Walton, D.B. 2004. Stochasticity, invasions, and branching random walks. *Theor. Pop. Biol.*, **66**: 174–184.
- Lewis, M.A. and Kareiva, P. 1993. Allee dynamics and the spread of invading organisms. *Theor. Popul. Biol.*, **43**: 141–158.
- Lewis, M.A. and Pacala, S.W. 2000. Modeling and analysis of stochastic invasion processes. *J. Math. Biol.*, **41**: 387–429.
- Lonsdale, W.M. 1999. Global patterns of plant invasions and the concept of invasibility. *Ecology*, **80**: 1522–1536.
- Matsuda, H., Tamachi, N., Ogita, A. and Sasaki, A. 1987. A lattice model for population biology. In *Mathematical Topics in Biology* (E. Teramoto and M. Yamaguti, eds.), pp. 154–161. Lecture Notes in Biomathematics Vol. 71. New York: Springer.
- McKane, A.J. and Newman, T.J. 2004. Stochastic models in population biology and their deterministic analogs. *Phys. Rev. E*, **70**: 041902 (19 pages).
- Murray, J. D. 2002. *Mathematical Biology*, 3rd edn. New York: Springer.
- Neubert, M.G., Kot, M. and Lewis, M.A. 2000. Invasion speeds in fluctuating environments. *Proc. R. Soc. Lond. B*, **267**: 1603–1610.
- Oborny, B., Meszena, G. and Szabo, G. 2005. Dynamics of populations on the verge of extinction. *Oikos*, **109**: 291–296.
- O'Malley, L., Allstadt, A., Korniss, G. and Caraco, T. 2005. Nucleation and global time scales in ecological invasion under pre-emptive competition. In *Fluctuations and Noise in Biological*,

- Biophysical, and Biomedical Systems III* (N.G. Stocks, D. Abbott and R.P. Morse, eds.), pp. 117–124. Bellingham, WA: SPIE.
- O'Malley, L., Basham, J., Yasi, J.A., Korniss, G., Allstadt, A. and Caraco, T. 2006a. Invasive advance of an advantageous mutation: nucleation theory. *Theor. Pop. Biol.*, **70**: 464–478.
- O'Malley, L., Kozma, B., Korniss, G., Rácz, Z. and Caraco, T. 2006b. Fisher waves and front roughening in a two-species invasion model with preemptive competition. *Phys. Rev. E*, **74**: 041116 (7 pages).
- O'Malley, L., Kozma, B., Korniss, G., Rácz, Z. and Caraco, T. in press. Fisher waves and the velocity of front propagation in a two-species invasion model with preemptive competition. In *Computer Simulation Studies in Condensed Matter Physics XIX* (D.P. Landau, S.P. Lewis and H.-B. Schüttler, eds.). Heidelberg: Springer.
- Pimentel, D., Lach, L., Zuniga, R. and Morrison, D. 2000. Environmental and economic costs of nonindigenous species in the United States. *Bioscience*, **50**: 53–65.
- Pimm, S.L. 1987. The snake that ate Guam. *Trends Ecol. Evol.*, **2**: 293–295.
- Ramos, R.A., Rikvold, P.A. and Novotny, M.A. 1999. Test of the Kolmogorov-Johnson-Mehl-Avrami picture of meta-stable decay in a model with microscopic dynamics. *Phys. Rev. B*, **59**: 9053–9069.
- Rikvold, P.A., Tomita, H., Miyashita, S. and Sides, S.W. 1994. Metastable lifetimes in a kinetic Ising model: dependence on field and system size. *Phys. Rev. E*, **49**: 5080–5090.
- Rosenzweig, M.L. 2001. The four questions: what does the introduction of exotic species do to diversity? *Evol. Ecol. Res.*, **3**: 361–371.
- Satō, K. and Iwasa, Y. 2000. Pair approximations for lattice-based ecological models. In *The Geometry of Ecological Interactions* (U. Dieckmann, R. Law and J.A.J. Metz, eds.), pp. 341–358. Cambridge: Cambridge University Press.
- Sax, D.F. and Brown, J.H. 2000. The paradox of invasion. *Global Ecol. Biogeogr.*, **9**: 361–371.
- Shea, K. and Chesson, P. 2002. Community ecology theory as a framework for biological invasions. *Trends Ecol. Evol.*, **17**: 170–176.
- Shurin, J.B., Amarasekare, P., Chase, J.M., Holt, R.D., Hoopes, M.F. and Leibold, M.A. 2004. Alternative stable states and regional community structure. *J. Theor. Biol.*, **227**: 359–368.
- Simberloff, D. 2000. Foreword. In *The Ecology of Invasions by Animals and Plants* (C.S. Elton, ed.), pp. vii–xiv. Chicago, IL: University of Chicago Press.
- Sintes, T., Marbà, N., Duarte, C.M. and Kendrick, G.A. 2005. Nonlinear processes in seagrass colonization explained by simple clonal growth rules. *Oikos*, **108**: 165–175.
- Tainaka, K. 2003. Lattice model for the Lotka-Volterra system. *J. Phys. Soc. Japan*, **57**: 2588–2590.
- Tainaka, K., Kushida, M., Itoh, Y. and Yoshimura, J. 2004. Interspecific segregation in a lattice ecosystem with intraspecific competition. *J. Phys. Soc. Japan*, **73**: 2914–2915.
- ter Horst, J.H. and Kashchiev, D. 2003. Determination of the nucleus size from the growth probability of clusters. *J. Chem. Phys.*, **119**: 2241–2246.
- Thomson, N.A. and Ellner, S.P. 2003. Pair-edge approximation for heterogeneous lattice models. *Theor. Popul. Biol.*, **64**: 271–280.
- Travis, J.M.J., Hammershøj, M. and Stephenson, C. 2005. Adaptation and propagule pressure determine invasion dynamics: insights from a spatially explicit model for sexually reproducing species. *Evol. Ecol. Res.*, **7**: 37–51.
- van Baalen, M. and Rand, D.A. 1998. The unit of selection in viscous populations and the evolution of altruism. *J. Theor. Biol.*, **193**: 631–648.
- van den Bosch, F., Hengeveld, R. and Metz, J.A.J. 1992. Analysing the velocity of animal range expansion. *J. Biogeogr.*, **19**: 135–150.
- van Saarloos, W. 2003. Front propagation into unstable states. *Phys. Rep.*, **386**: 29–222.
- Veltman, C.J., Nee, S. and Crawley, M.J. 1996. Correlates of introduction success in exotic New Zealand birds. *Am. Nat.*, **147**: 542–557.

- White, A., Greenman, J.V., Bentob, T.G. and Boots, M. 2006. Evolutionary behaviour in ecological systems with trade-offs and non-equilibrium population dynamics. *Evol. Ecol. Res.*, **8**: 387–398.
- Yasi, J.A., Korniss, G. and Caraco, T. 2006. Invasive allele spread under preemptive competition. In *Computer Simulation Studies in Condensed Matter Physics XVIII* (D.P. Landau, S.P. Lewis and H.-B. Schüttler, eds.), pp. 165–169. Heidelberg: Springer.
- Yoshimura, J., Tainaka, K., Suzuki, T., Sakisaka, Y., Nakagiri, N., Togashi, T. *et al.* 2006. The role of rare species in the community stability of a model ecosystem. *Evol. Ecol. Res.*, **8**: 629–642.
- Zadoks, J.-C. 2000. Foci, small and large: a specific class of biological invasion. In *The Geometry of Ecological Interactions* (U. Dieckmann, R. Law and J.A.J. Metz, eds.), pp. 292–317. Cambridge: Cambridge University Press.

### APPENDIX 1

We obtain an approximate expression for  $m(2)$  in the limit where  $r/R \ll 1$ . To that end, we use an asymptotic small-argument,  $z \equiv (r/2R)$ , as well as using the following expansions for the non-linear functions appearing in equation (4):

$$\arcsin(z) = z + \frac{z^3}{6} + O(z^5)$$

and

$$\sqrt{1-z^2} = 1 - \frac{z^2}{2} + O(z^4)$$

For  $m(2)$ , we find:

$$\begin{aligned} m(2) &= \pi r^2/2 + 2R^2(1-2z^2)\arcsin(z) - 2R^2z\sqrt{1-z^2} \\ &= \pi r^2/2 + R^2 \left[ 2(1-2z^2) \left( z + \frac{z^3}{6} + O(z^5) \right) - 2z \left( 1 - \frac{z^2}{2} + O(z^4) \right) \right] \quad (\text{A1.1}) \\ &= \pi r^2/2 + R^2 [-8z^3/3 + O(z^5)] \approx \pi r^2/2 - R^2 8/3 \left( \frac{r}{2R} \right)^3 \\ &= \pi r^2/2 \left[ 1 - \left( \frac{2}{3\pi} \right) \left( \frac{r}{R} \right) \right] \end{aligned}$$

Since  $m(1) = \pi r^2 - m(2)$ , we have:

$$m(1) = \pi r^2/2 \left[ 1 + \left( \frac{2}{3\pi} \right) \left( \frac{r}{R} \right) \right] \quad (\text{A1.2})$$

### APPENDIX 2

A mean-field approximation to a spatial model assumes homogeneous mixing, so that spatial correlations do not influence the dynamics (Duryea *et al.*, 1999; Yoshimura *et al.*, 2006). The mean-field approximation to our individual-based model has dynamics:

$$d\rho_i/dt = \alpha_i \rho_i (1 - \rho_1 - \rho_2) - \mu_i \rho_i; \quad i = 1, 2 \quad (\text{A2.1})$$

where  $\rho_i$ ,  $0 \leq \rho_i \leq 1$ , is (in the mean-field model) the global density of species  $i$ ;  $i = 1, 2$ . Assume for simplicity  $\mu_1 = \mu_2 = \mu$ . Since  $\alpha_i > \mu$  for both species, mutual extinction cannot be

stable. In the absence of species  $j$ , the stable mean-field equilibrium density of species  $i$  is  $\rho_i^* = 1 - (\mu/\alpha_i)$  (Korniss and Caraco, 2005; O'Malley *et al.*, 2006a).

In the context of critical cluster size, we do not assume global mixing. Rather, we assume that  $\rho_1^*$  gives densities in the area surrounding the invader cluster (where only residents occur), and that  $\rho_2^*$  gives densities within the invader cluster (where no residents occur). Applying the mean-field densities to the continuous-space model, equation (5) of the text becomes:

$$m(2) = \pi r^2 \frac{\alpha_1 - \mu}{\alpha_1 + \alpha_2 - 2\mu} \quad (\text{A2.2})$$

at  $R = R_{\text{crit}}$ . By inspection,  $\partial m(2)/\partial \alpha_1 > 0$  and  $\partial m(2)/\partial \alpha_2 < 0$ . Then  $R_{\text{crit}}$  varies directly (inversely) with the resident's (invader's) propagation rate. From (A2.2):

$$\partial m(2)/\partial \mu = \pi r^2 (\alpha_1 - \alpha_2)/(\alpha_1 + \alpha_2 - 2\mu)^2 \quad (\text{A2.3})$$

The critical radius should vary with  $\mu$  according to the sign of  $(\alpha_1 - \alpha_2)$ . The invader has the greater propagation rate, and an increase in the common mortality rate should decrease the critical radius.

Pair approximation for lattice models tracks the deterministic dynamics of both global densities and local densities conditioned on the state of a neighbouring site (Dickman, 1986; Matsuda *et al.*, 1987). By incorporating correlations of nearest neighbours into the dynamics, pair approximation may predict equilibrium densities more accurately than mean-field models (Ellner *et al.*, 1998; Bauch and Rand, 2000; Satō and Iwasa, 2000; Tainaka, 2003; Caraco *et al.*, 2006).

In the pair approximation to our spatial model, the stable equilibrium density of species  $i$ , in the absence of species  $j$ , is:

$$\rho_i^* = \frac{\delta - 1 - \delta(\mu/\alpha_i)}{\delta - 1 - (\mu/\alpha_i)}, \quad i = 1, 2 \quad (\text{A2.4})$$

Using equation (5), we have:

$$m(2) \propto \frac{\alpha_1(\delta - 1) - \delta\mu}{(\alpha_1 + \alpha_2)(\delta - 1) - 2\delta\mu} \quad (\text{A2.5})$$

Differentiation again shows that the sign of  $\partial m(2)/\partial \mu$  has the sign of  $(\alpha_1 - \alpha_2)$ , and so the critical radius should decline with increased mortality.